AIMS Geosciences

AIMS Geosciences, 9(1): 34–48.
DOI: 10.3934/geosci.2023003
Received: 14 November 2022
Revised: 22 November 2022
Accepted: 28 November 2022
Published: 05 December 2022

http://www.aimspress.com/journal/geosciences

Research article

Density investigation and implications for exploring iron-ore deposits using gravity method in the Hamersley Province, Western Australia

William Guo*

School of Engineering and Technology, Central Queensland University, North Rockhampton QLD 4702, Australia

* **Correspondence:** Email: w.guo@cqu.edu.au; Tel: 61749309687.

Abstract: The Hamersley Province in the northwest of Western Australia contains extensive banded iron formations (BIFs) and large hematite-goethite deposits. Density information of rocks and ores in this region has been scarce. This study reports the results of a systematic density investigations based on more than eight hundred density datasets in the province. This study not only provides a better understanding of density distribution of the rocks and ores in the province, but also allows forward gravity modeling over the known iron-ore deposits to be conducted for exploring the usefulness and effectiveness of gravity surveys for detecting concealed iron-ore deposits in the region. This should have a significant impact on iron-ore mining in the province as the outcropped ores have been mined for over 40 years in the province and the future targets are likely the concealed deposits below the surface. The analysis shows a clear density contrast around 1.0 g/cm^3 between the Brockman iron ores and the host BIFs, which should generate clear positive net gravity anomalies over buried large iron-ore deposits. However, porous goethite ores hosted in the Marra Mamba BIFs have an average density of about 2.8 g/cm^3 due to porosity about 30–40% in the ores. A density contrast of −0.5 g/cm^3 may exist between the goethite ores and BIFs, which would produce net negative gravity anomalies over the deposits. Since most goethite deposits are layered consistently with the host rocks and associated with broad folds, the net gravity anomaly of an orebody itself may generally have the similar shape to the corresponding BIF bedrock. This implies that gravity surveys may be able to detect paleochannels which host the goethite ores, rather than directly detecting the orebody.

Keywords: Hamersley Province; iron ores; bulk density of rocks and ores; banded iron formation (BIF); forward gravity modeling; iron-ore exploration

1. Introduction

The Hamersley Province in the southern Pilbara Block is situated in the northwest of Western Australia, about 1,000 km north of Perth (Figure 1). It is about 500 km long and 250 km wide, with a west-north-westerly elongation [1–6]. The region is mountainous and arid. The Hamersley Province is defined by the extent of the Hamersley Group of sedimentary and volcanic rocks and contains extensive banded iron formations (BIFs) and large hematite-goethite deposits. It is one of the major iron-ore producers in the world.

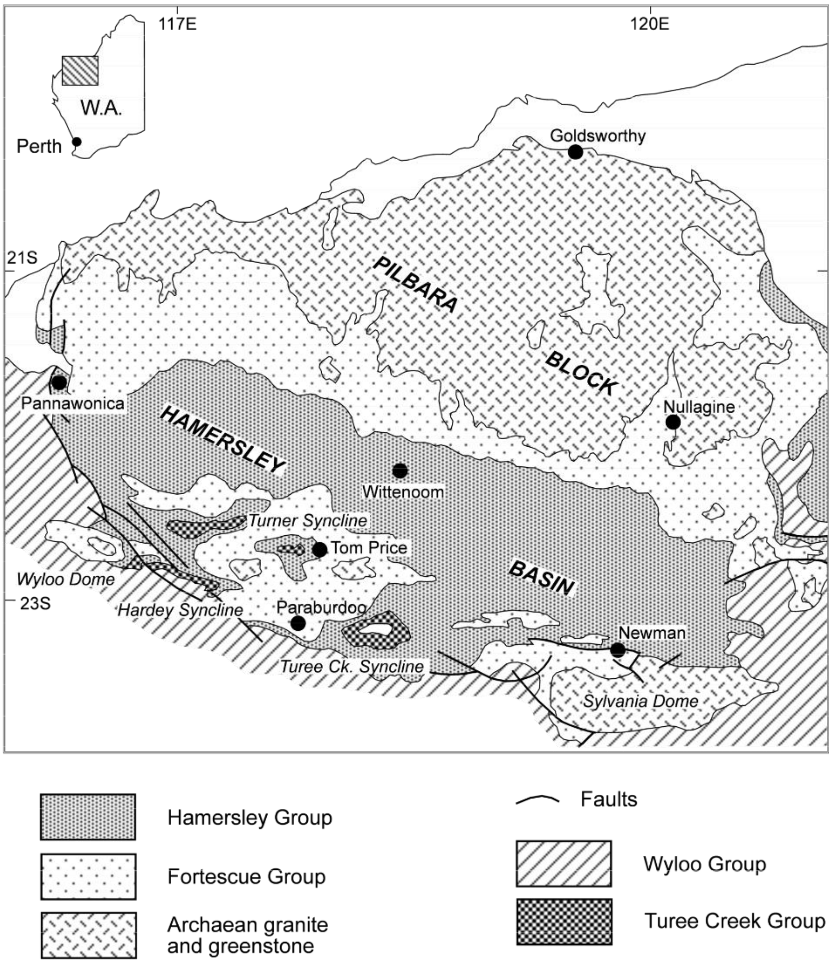

Figure 1. Simplified geological map of the Hamersley Province.

The BIF-derived high-grade hematite-goethite deposits have been a paradox for geophysical exploration. BIFs usually produce strong magnetic anomalies, from which geophysicists and geologists can easily approach the target areas. On the other hand, how to accurately determine the anomaly caused by high-grade iron ores, which is often much less magnetic than BIFs and trapped in the huge magnetic "sea" dominated by BIFs' contribution, remains problematic. The Hamersley Province is in the same dilemma. Geophysical methods have been tried in the Hamersley Province since late 1990s [7,8], but the effectiveness of geophysical methods is constrained by many factors, such as a lack of systematic petrophysical data to support detailed geophysical interpretation, despite the availability of some magnetic petrophysical data resulted from different projects since 1960s [9–11]. Since BIFs are much stronger in magnetic responses compared with the high-grade hematite-goethite ores, interpretation of magnetic survey data is further complicated by anisotropy in magnetic susceptibility and possibly in remanent magnetization, self-demagnetization, magnetization related to pre-folding or post-folding, etc. [2,10–13], which limits magnetic methods, either ground or airborne, as qualitative meanings in iron-ore exploration.

Owing to the significant difference in density between the high-grade hematite ores and BIFs (and other rock units), gravity survey may have an immense potential in exploring concealed iron-ore deposits in the region, subject to the availability of a comprehensive density database for the rocks and ores in the region. In the Hamersley Province, only a few density data for selected rock units and iron ores were mentioned in public [14–17] until the early 2000s when a set of density data was cited in [18] for regional gravity data modeling in the west of the Hamersley Province. However, the details of this density investigation and applications for exploring potential iron-ore deposits were not disclosed due to confidentiality and other issues. In this paper, the systematic density investigation in the province, based on more than eight hundred density measurements from over one thousand specimens that cover all the geological units in the province, is reported, followed by forward gravity modeling over two known iron-ore deposits in the province for assessing the effectiveness of gravity method for future iron-ore exploration.

The rest of this paper is organized as follows. Section 2 outlines the geological background of the Hamersley Province. Methods in sampling, density measurement and data statistics are summarized in Section 3. The results of bulk density for rock units and ore types resulted from this density investigation for the province are presented in Section 4. Section 5 discusses implications of the density results on the forward gravity modeling and the effectiveness of the forward gravity modeling for exploring different types of iron-ore deposits. Brief conclusions are drawn for this study in Section 6.

2. Geological background

Archaean granite-greenstone outcrops over most of the northern half of the Pilbara Block and is unconformably overlain by the Hamersley Basin in the southern half of the block except a few exposures in inliers or domes in the basin (Figure 1). There are three major stratigraphic units aged from the Late Archaean to the Early Proterozoic within the basin, i.e., in ascending order, the Fortescue, Hamersley and Turee Creek Groups (Figure 2), which are collectively referred to as the Mount Bruce Supergroup. Hamersley Basin rocks are unconformably overlain to the south by the Ashburton Basin. Most rocks of the Hamersley and Ashburton Basins have been subjected to greenschist facies metamorphism.

The Fortescue Group is the lowermost stratigraphic unit of the Hamersley Basin and rests with angular unconformity upon granite-greenstone basement. The Fortescue Group is up to 1.8 km thick and consists of low-grade metamorphosed volcanic and sedimentary rocks.

The Hamersley Group conformably overlies the Fortescue Group and is conformably overlain by the Turee Creek Group. It is approximately 2.5 km thick and consists of five important iron formations separated by sequences of dolomites, shales and volcanics. The Hamersley Group is divided, in ascending order, into the following eight formations: Marra Mamba Iron Formation, Wittenoom Dolomite, Mount Sylvia Formation, Mount McRae Shale, Brockman Iron Formation, Weeli Wolli Formation, Woongarra Rhyolite, and Boolgeeda Iron Formation. Most of the iron ore deposits occur in the Brockman Iron Formation, approximately 620 m thick, and the Marra Mamba Iron Formation, approximately 230 m thick although both the Weeli Wolli Formation and Boolgeeda Iron Formation also contain minor enrichments. The Marra Mamba Iron Formation has been subdivided into three members: Nammuldi, MacLeod, and Mount Newman Members. The Brockman Iron Formation consists of four members: Dales Gorge, Whaleback Shale, Joffre and Yandicoogina Shale Members.

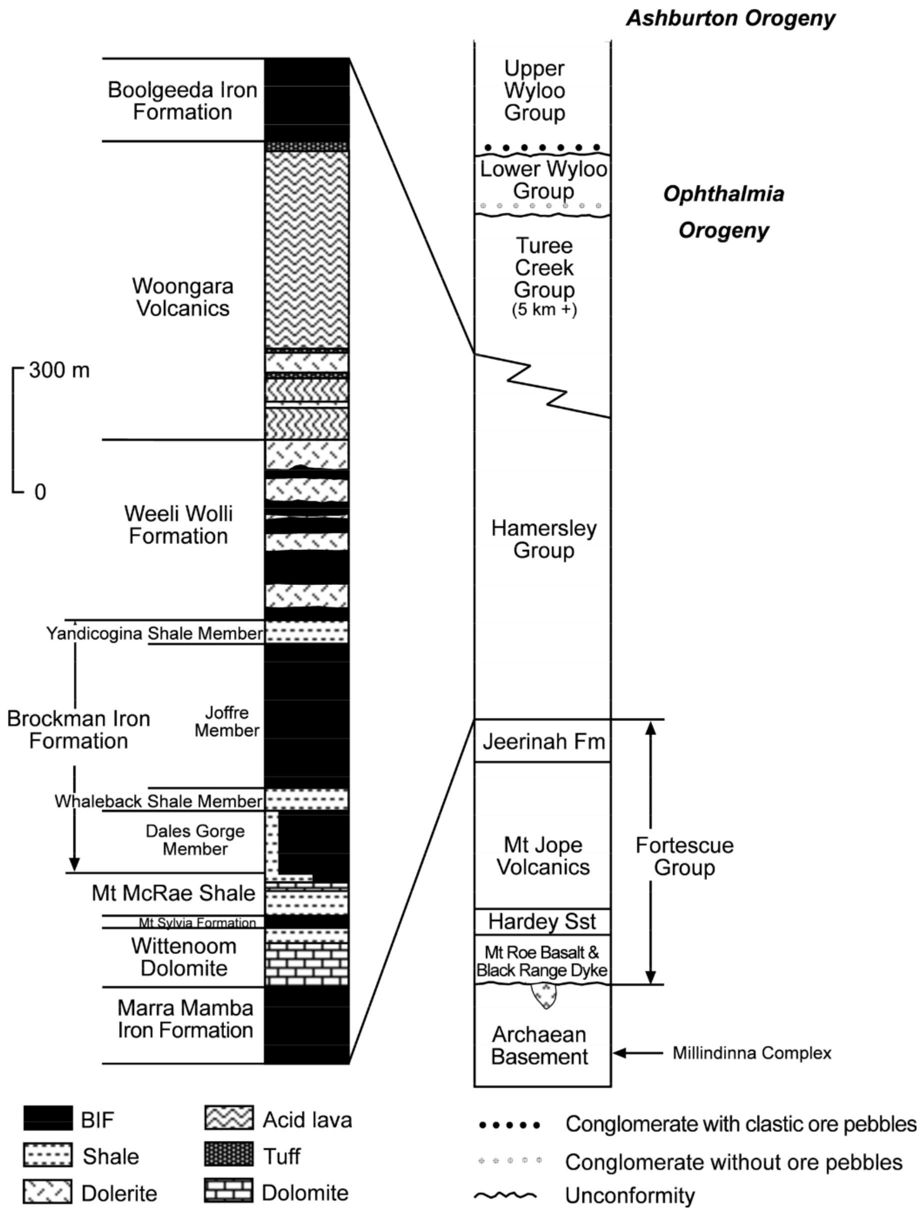

Figure 2. Stratigraphy in the Hamersley Province.

The Turee Creek Group conformably overlies the Boolgeeda Iron Formation and comprises fine-grained to coarse-grained siliclastic rocks with locally developed chemical deposits. The Wyloo Group unconformably overlies the Mount Bruce Supergroup with a maximum thickness of approximately 10–12 km, and is subdivided, in ascending order, into: Beasley River Quartzite, Cheela Springs Basalt, Mount McGrath Formation, Duck Creek Dolomite, and Ashburton Formation.

More detailed information about the geology and classification of iron ores in the Hamersley Basin can be found in the classical works in [1,19–21], and recent studies reported in [22–24].

3. Sampling, density measurement and data statistics

A total of 574 samples were collected from three field trips over the Hamersley Province and the stratigraphic distribution of these samples is summarized in Table 1. More than one thousand measurement specimens were prepared, from which 873 independent density measurements were taken, which covered most of the stratigraphic units and iron ores in the Hamersley Province.

Table 1. Samples and stratigraphic distribution.

Group	Formation	Sampling site	Number of samples	Lithology
	Duck Creek Dolomite	2	10	Dolomite, sandstone
Wyloo	Mount McGrath	1	6	Hematite conglomerate
	Cheela Spring Basalt	2	9	Basalt
Turee Creek		2	17	Dolomite
	Boolgeeda	6	38	BIF, siltstone
	Woongarra Rhyolite	3	18	Rhyolite
	Weeli Wolli	6	27	BIF
Hamersley	Brockman	46	205	BIF, iron ore
	Mount McRae Shale	1	9	Shale, dolomite
	Mount Sylvia	8	28	BIF
	Wittenoom Dolomite	13	76	Dolomite
	Marra Mamba	11	50	BIF, chert, iron ore
Fortescue		11	69	Basalt, pillow lava
	Dyke	2	6	Dolerite

The density commonly used in geophysical modeling is the dry bulk density—the ratio of the dry rock mass to the total of the volumes of the rock material and pores, i.e., the bulk volume of the rock sample. In this study the dry bulk density (hereafter as bulk density or density) of 873 specimens from the province were measured using a Shimadzu electronic balance with sensitivity about 0.1 mg by means of the wet method described in [25,26]. The bulk density (σ) is calculated by formula

$$\sigma = \frac{W_{da}}{W_{da} - W_w} \tag{1}$$

where W_{da} is the weight of the dry sample measured in air; W_w is the weight of the same sample measured in water.

All measurements for a rock unit or ore type were subject to the normal distribution test. As all rock units and ore types showed normal or near normal distributions in density (Figure 3), arithmetic mean and corresponding standard deviation were calculated based on each of the rock and ore types. The Fortescue Group is treated as one unit because it shows the wide homogeneity in density.

4. Bulk density of rock types and iron ores in the Hamersley province

4.1. Bulk density of BIF units

The average density for all BIF units varies from 3.1 to 3.4 g/cm^3 (Table 2) with an overall average of 3.25 g/cm^3 (Table 3). The average density for a BIF unit depends on the degree of oxidization and/or iron concentration of the samples collected from that BIF unit. Some BIF samples collected from surfaces with visible oxidization and less iron contents can be lighter than dolomite whereas those heavily mineralized BIF units within Marra Mamba, Brockman, and Boolgeeda Iron Formations can be as heavy as the iron ores (Table 2).

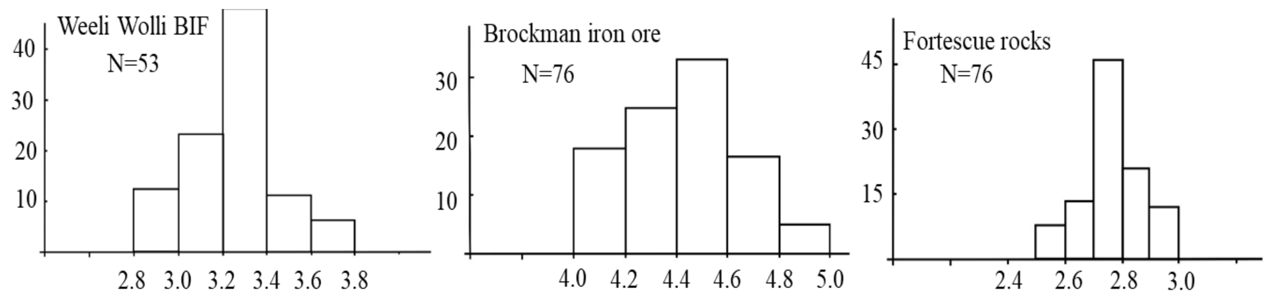

Figure 3. Samples of normal and near normal distributions of rock units and iron ores.

Table 2. Mean density of geological units.

Formation/Member	n	Mean density (g/cm^3)		
		σ	S.D.	Range
Duck Creek Dolomite	25	2.724	0.070	2.620–2.880
Cheela Springs Basalt	21	2.755	0.040	2.695–2.848
Turee Creek Dolomite	20	2.858	0.030	2.772–2.895
Boolgeeda Iron Formation	42	3.405	0.648	2.609–4.639
Woongarra Rhyolite	33	2.652	0.019	2.625–2.687
Weeli Wolli Formation	53	3.228	0.242	2.703–3.556
Brockman Iron Formation (BIF)	195	3.398	0.411	2.557–4.541
Mount McRae Shale	10	2.518	0.162	2.243–2.737
Mount Sylvia BIF	43	3.156	0.266	2.563–3.615
Wittenoom Dolomite	90	2.836	0.081	2.557–2.934
Marra Mamba Iron Formation	52	3.105	0.367	2.418–4.084
Fortescue Group	76	2.763	0.110	2.450–2.775

4.2. Bulk density of iron ores

The average density for the martite-hematite ores hosted in the Brockman Iron Formation (or the Brockman ores) is 4.4 g/cm^3 (Table 3), ranging from 4.2 g/cm^3 to 4.7 g/cm^3. Note this was mainly resulted from the iron-rich bands within the iron-ore deposits. This average would be lower if considering the proportion of the iron-poor bands within the deposits. Iron ores hosted in the Marra

Mamba Iron Formation have two different types depending on where the ores are located. The condensed ores under the "hard-cap" are rich in martite with a lower proportion of porous goethite. Hence, such condensed martite-goethite ores below the hard-cap have an average density of around 4.0 g/cm^3, varying from 3.5 g/cm^3 to 4.4 g/cm^3. The goethite-rich ores further below the condensed martite-goethite ores are much lighter with an average density of 2.85 g/cm^3, ranging from 2.8 g/cm^3 to 3.25 g/cm^3.

Table 3. Mean density of rock types and iron ores.

Rock type and iron ore	Mean density (g/cm^3)
BIFs	3.250
Brockman Martite-hematite ores	4.425
Marra Mamba martite-goethite ores	
Condensed martite-rich ores (below the hard-cap)	4.011
Goethite-rich ores	2.850
Dolomite	2.806
Shale	2.518
Rhyolite	2.652
Basalt	2.761
Dolerite	2.876
Archaean granite [27]	2.640

4.3. Bulk density of other rocks

Dolerite dykes have an average density of 2.876 g/cm^3 (Table 3). Turee Creek dolomite has a very similar average density of 2.858 g/cm^3 to that of 2.836 g/cm^3 for the Wittenoom Dolomite. Both of them are slightly higher than the Duck Creek Dolomite with an average density of 2.724 g/cm^3. The average of all dolomites is 2.8 g/cm^3 (Table 3). Basalt dominated Fortescue rocks have an average density of 2.763 g/cm^3, similar to that of 2.755 g/cm^3 for the Cheela Springs Basalt. The average density for basalts is 2.761 g/cm^3. Woongarra Rhyolite has an average density of 2.652 g/cm^3, which is very similar to that of the Archaean granite with 2.640 g/cm^3 (Table 3). Mount McRae Shale seems to be the lightest rock type with an average density of 2.518 g/cm^3 in all the rocks in the Hamersley Province.

5. Discussion and forward gravity modeling

5.1. Bulk density, porosity and hematite content of iron ores

By quantitative XRF analysis of forty-three BIF and ore samples, the iron content in these samples were determined as the weight percentage of Fe2O3 [2]. A linear regression between the weight percentage of Fe2O3 (W) and bulk density was determined with a correlation coefficient of 0.931 by the following relationship (Figure 4).

$$\sigma = 0.0215W + 2.2224. \quad (2)$$

Ideally, assuming a sample only contains pure hematite, its density resultant from equation (2) would be 4.36 g/cm^3, which is much less than the mineral density (5.3 g/cm^3) of hematite [28]. From XRD analysis [2], even for those ore samples containing 99.8% hematite, the maximum density is only 4.56 g/cm^3. This lower bulk density may be mainly due to the porosity in the ores. Gilhome [17] and Aylmer et al [29] reported that the range of porosity was from 4% to 28% for the Hamersley hematite ores, and 25% to 48% for goethitic shales. A porosity value of 19% could be regarded as a reasonable average for typically condensed martite-hematite ores whereas the more porous goethite ores could have a porosity of about 30–40% [29].

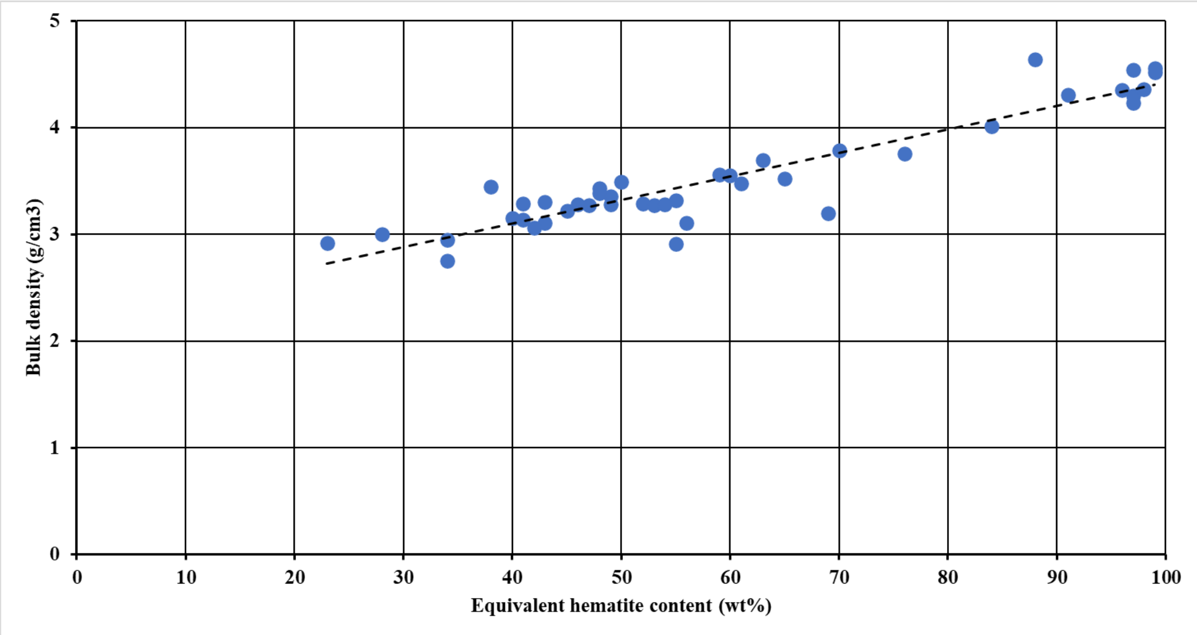

Figure 4. Linear regression between bulk density and equivalent hematite content (wt%) by XRF analysis of selected BIF and iron-ore samples from the Hamersley Province.

According to [30], relationship between the bulk density and porosity (ϕ) of a sample can be determined by

$$\sigma = (1 - \phi)\cdot\sigma_m + \phi\cdot\sigma_p, \tag{3}$$

where σ_m is the mean density of the solid matrix material; σ_p is the mean density of material filled in pores. Assuming the ores are dominated by hematite with the mineral density of 5.3 g/cm^3 and pores are filled with air, the average bulk density of martite-hematite ores having a mean porosity of 19% should be about 4.3 g/cm^3. This value is close to the mean density of the Brockman ores (4.4 g/cm^3), and similar to the value determined from equation (2). As higher porosity would be expected for Marra Mamba ores, martite-rich ores may have a mean density of about 4.0 g/cm^3 whereas goethite-rich ores may have an average density of about 2.85 g/cm^3 (Table 3).

5.2. Weathering effect on density variation of BIFs

Assuming the pores in BIFs are filled with air, the porosity of the BIF samples can be estimated by means of the following formula [26].

$$\phi = \frac{W_{sa} - W_{da}}{W_{sa} - W_{sw}}, \tag{4}$$

where W_{da} is the weight of the dry sample measured in air; W_{sa} is the weight of the water-saturated sample measured in air; W_{sw} is the weight of the water-saturated sample measured in water. The solid BIF samples, physically similar to the fresh BIFs, could have a porosity below 1%. Porosity of other weathered BIFs varies from 1.6% to 8.6% with a mean value of 4% (Table 4), which is similar to that of the most condensed hematite ores.

According to [14,15], the average density of fresh BIF-bands in the Dales Gorge Member was 3.5 g/cm^3, and the whole member-mean density (BIF bands + shale bands) was 3.4 g/cm^3. The average density of fresh BIF-bands in the Marra Mamba Iron Formation was 3.2 g/cm^3, and the whole formation mean density (BIF bands + shale bands) was 3.1 g/cm^3.

Table 4. Porosity of surface BIF samples from the Hamersley Province.

Sample	Porosity (%)	Formation Average (%)	Overall Average (%)
Boolgeeda 1	5.65	4.61	4.05
Boolgeeda 2	3.96		
Boolgeeda 3	4.22		
Weeli Willi 1	4.77	5.21	
Weeli Willi 2	1.60		
Weeli Willi 3	2.32		
Weeli Willi 4	5.96		
Weeli Willi 5	8.03		
Weeli Willi 6	8.58		
Brockman 1	0.29	0.27	
Brockman 2	0.18		
Brockman 3	0.27		
Mount Sylvia 1	4.07	3.77	
Mount Sylvia 2	3.33		
Mount Sylvia 3	3.90		
Marra Mamba 1	2.61	5.25	
Marra Mamba 2	6.80		
Marra Mamba 3	6.35		

The surface weathering makes the parent magnetic minerals (magnetite + hematite) in BIFs chemically changed from denser magnetite (5.2 g/cm^3) to maghemite (5.1 g/cm^3) and finally to lighter goethite (4.3 g/cm^3) [19,29]. At the same time, porosity in BIFs increases with weathering. As a result, the resultant mean densities of most BIF samples collected from the natural outcrops would be still lower than those of fresh BIF samples around 3.4 g/cm^3, similar to those of the whole member-mean and/or formation-mean densities of iron formations, for example, the mean density of 3.4 g/cm^3 for the whole Dales Gorge Member. Considering the fact that the Dales Gorge Member is the most iron-rich unit among all BIF units, an equivalent average density for all BIF units in the Hamersley Province around 3.2 g/cm^3 would be a reasonable estimate for the purpose of gravity modeling.

5.3. Forward gravity modeling over iron-ore deposits in the Hamersley Province

Although no real gravity data around mines are available for modeling, forward modeling can be conducted over two real iron-ore deposits using the systematic density data obtained in this study. The modeling profiles were the cross-sections of real open-pits of iron-ore deposits. The forward modeling can provide some insights for future explorations of concealed iron-ore deposits in the Hamersley Province.

The profile in Figure 5 was from a hematite deposit hosted in the Brockman Iron Formation. Considering the impurity of the ores and compositions of iron-rich, iron-poor, and shale bands within a BIF unit around this site, the following average densities were assigned for the geological units for the modeling: 3.9 g/cm^3 for iron-ores as the bottom estimate, 3.2 g/cm^3 for the fresh and unmineralized BIFs, 2.8 g/cm^3 for dolomite and Fortescue basalts, 2.9 g/cm^3 for dolerite dykes and BIF-shale mixed Mount Sylvia Formation and 2.5 g/cm^3 for shales.

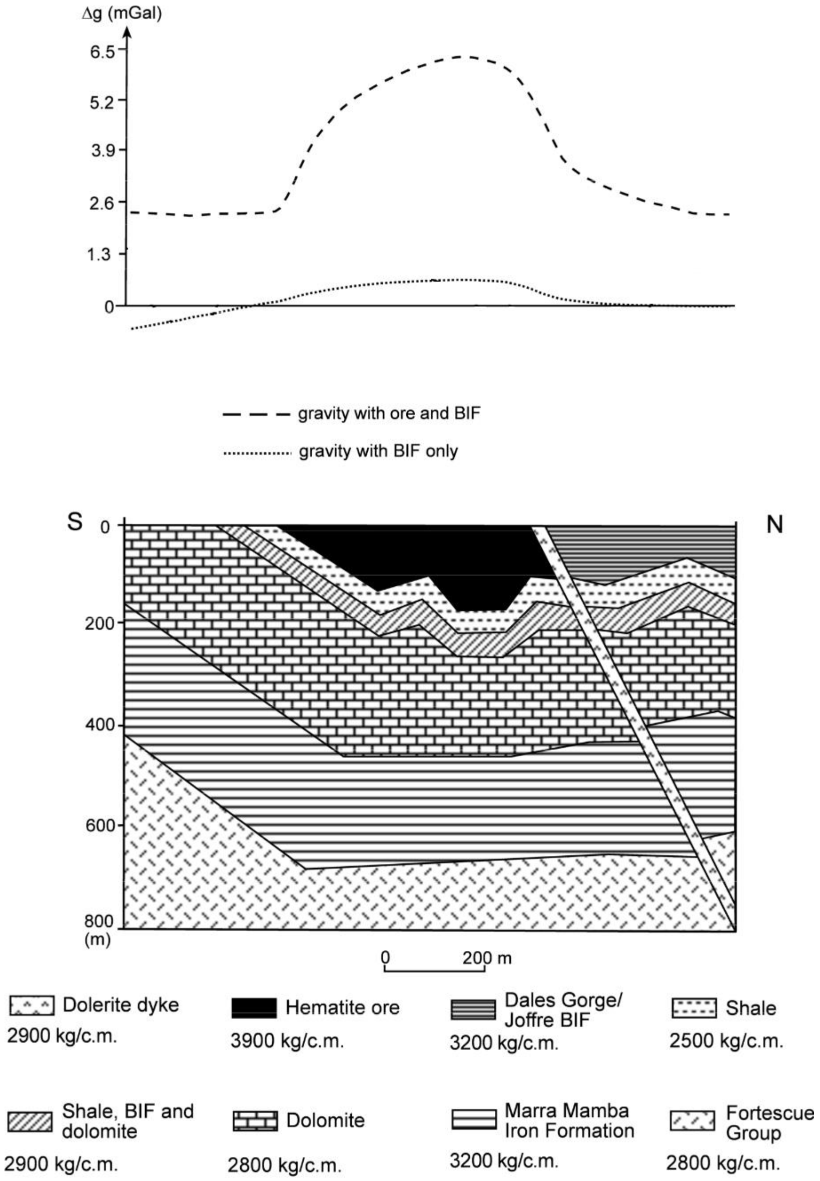

Figure 5. Gravity modeling over a hematite deposit in the Hamersley Province.

Taking the exposures of the Fortescue Group as the reference, a residual gravity anomaly of about +6.5 mGal appears over the orebody (dash line). If the density for the orebody is replaced by the density for unmineralized BIFs, there would be a very small gravity anomaly of about +1.0 mGal (dot line) appears over the place where the orebody should be. This means that the residual gravity anomaly over the orebody is mainly contributed by the denser martite-hematite ores. Since the density for the Brockman martite-hematite ores is usually around 4.4 g/cm^3, much higher than the bottom value of 3.9 g/cm^3 used for the forward modeling, detailed gravity surveys look likely to delineate Brockman martite-hematite deposits in the Hamersley Province, even concealed below the surface for 50–100 m due to the significant difference in density between the martite-hematite ores and the surrounding rocks in the region.

The profile in Figure 6 is a goethite-rich iron-ore deposit hosted in the Marra Mamba Iron Formation. The upper part of this formation was mineralized into goethite ores along an east-west paleochannel after supergene processes [19,21] whereas the lower unmineralized part formed the bedrock beneath the ores. Porous goethite ore itself may have a mean density of about 2.8 g/cm^3, but the interbedded shale layers within the ores make the equivalent mean density of the orebody down to about 2.6 g/cm^3. Moreover, in most cases there are Tertiary and/or Quaternary sediments sitting on top of the ore-bearing paleochannels. Thus, negative residual gravity anomalies or relative gravity lows are expected to occur over the orebodies or paleochannels. In such circumstances, differing from the condensed martite-hematite deposits, detecting paleochannel may lead to locate goethite deposits. A relative gravity low, referred to the Fortescue Group rocks, occurs over the goethite deposit (Figure 6). After taking a background field of 2.5 mGal, a residual anomaly of about −2.2 mGal, similarly to the variation of the bedrock surface, appears. This may imply that detailed high resolution gravity surveys may be useful in determining the goethite ore-hosting paleochannels, rather than detecting the deposit directly.

6. Conclusions

This study enables geoscientists and mining engineers to systematically understand the density distribution of almost all the geological units in the Hamersley Province for the first time. The martite-hematite ores hosted in the Brockman Iron Formation have an averaged bulk density of 4.4 ± 0.2 g/cm^3 and all the BIF units have an averaged bulk density of 3.2 ± 0.5 g/cm^3. Thus, a clear density contrast around 1.0 g/cm^3 exists between the martite-hematite ores and the host BIFs. The porous goethite-rich ores derived from the Marra Mamba BIFs have an averaged density of about 2.8 g/cm^3 due to the presence of porosity of 30–40% in the ores. An average density contrast of about −0.5 g/cm^3 exists between the goethite-rich ores and the host BIFs. Some fresh dolerite dykes have an average density of about 3.0 g/cm^3 whereas the widely distributed thick and flat Fortescue Group rocks and Archaean granites have an average density of about 2.8 ± 0.1 g/cm^3.

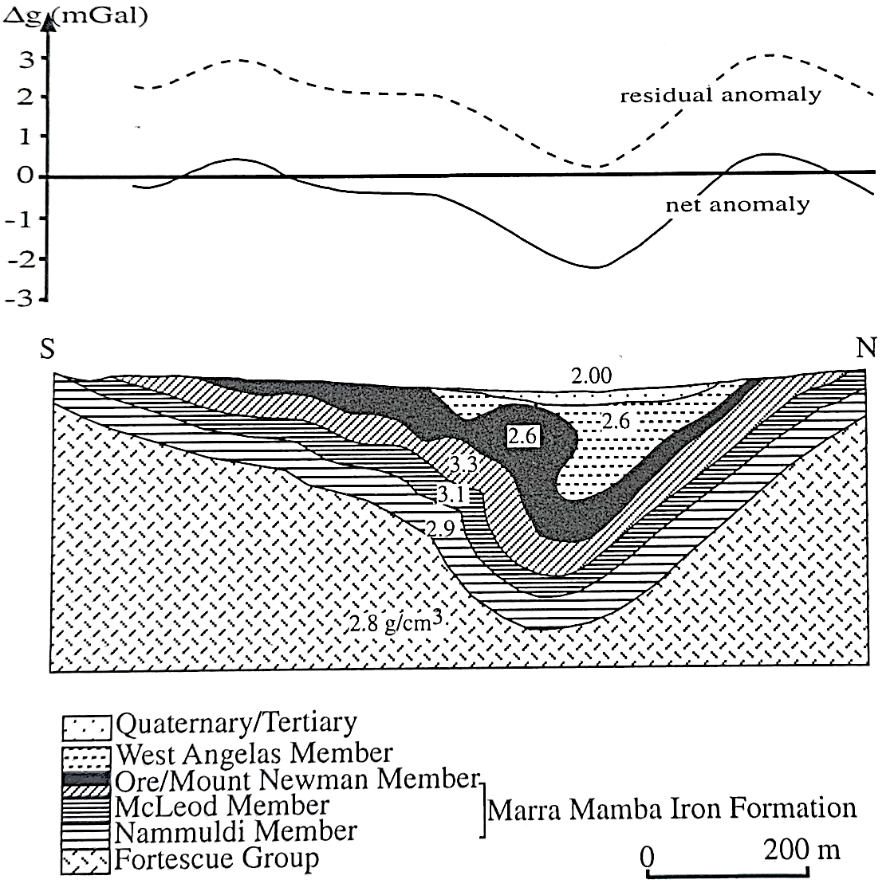

Figure 6. Gravity modeling over a goethite-rich deposit in the Hamersley Province.

For the martite-hematite deposits, significant positive residual gravity anomalies generated by the combination of the orebody and the hosting BIFs can be expected to occur over concealed large deposits with respect to the relatively flat and extensive outcrops of the Fortescue Group rocks and/or Archaean granite. Net gravity anomaly produced by the martite-hematite ores would dominate the residual gravity anomaly should the BIF host a large-scale orebody. For goethite-rich deposits, negative net gravity anomalies could occur over the deposits. As most goethite deposits are layered consistently with the host rocks and associated with broad folds, the net gravity anomaly of an orebody itself may generally have the similar shape to the corresponding BIF bedrock. Therefore, gravity surveys may be able to detect paleochannels which host the goethite ores. Given the fact that the interpretation of the magnetic survey data in the Hamersley Province is affected by many complicated factors, such as self-demagnetization, anisotropy of magnetic susceptibility, orientations of remanent magnetizations with respect to historical geological events, consistency in magnetism between surface and fresh BIFs, gravity survey may be more useful and effective for exploring concealed iron-ore deposits in the province.

However, the availability of a comprehensive density database of rocks and ores in the Hamersley Province is only the basis to help explore concealed large iron-ore deposits in the region through gravity survey. Innovative and/or collaborative methods must be considered in the inverse modeling of the gravity data, such as simulated annealing or combination with neural networks or genetic algorithms [31–34], to better deal with the nonlinear nature of inverse modeling.

Acknowledgments

Much of the original work was supported by the Minerals & Energy Research Institute of WA, BHP, Rio Tinto, and The University of Western Australia. Special thanks go to Professor Z-X Li for his guidance and help during the field trips and sample collections for a paleomagnetic project, which enabled this density investigation.

Conflict of interest

The author declares no conflict of interest.

References

1. Trendall AF (1983) The Hamersley Basin, In: Trendall A.F. and Morris R.C. Eds., *Iron—formation: facts and problems*, Elsevier, 69–129.
2. Guo WW (1999) *Magnetic petrophysics and density investigations of the Hamersley Province, Western Australia: implications for magnetic and gravity interpretation*, Australia, The University of Western Australia.
3. Li ZX, Guo W, Powell CMA (2000) *Timing and genesis of Hamersley BIF-hosted iron deposits: a new palaeomagnetic interpretation*. Perth, Australia, Minerals & Energy Research Institute of Western Australia.
4. Bodycoat FM (2010) Stratigraphic and structural setting of iron mineralization at E Deposit (East), Area C, Hamersley Province, Western Australia. *Appl Earth Sci* 119: 49–55. https://doi.org/10.1179/037174510X12853354810543
5. Geological Survey of Western Australia, *Fortescue–Hamersley: Extended abstracts*. Perth Australia: Geological Survey of Western Australia, 2022. Available from: https://dmpbookshop.eruditetechnologies.com.au/product/fortescuehamersley-2022-extended-abstracts.do.
6. Perring CS, Hronsky JMA, Crowe M (2022) Phanerozoic history of the Pilbara region: implications for iron mineralization. *Aust J Earth Sci* 69: 757–775. https://doi.org/10.1080/08120099.2022.2048888
7. Butt AL, Flis MF (1997) The application of geophysics to iron ore mining in the Hamersley Basin, Western Australia. *Explor Geophys* 28: 195–198. https://doi.org/10.1071/EG997195
8. Hawke PJ, Flis MF (1997) Application of electrical techniques for iron ore exploration. *Exploration Geophysics* 28: 242–246.
9. Porath H, Chamalaun FH (1968) Palaeomagnetism of Australian haematite ore bodies, II, Western Australia. *Geophys J R Astr Soc* 15: 253–264. https://doi.org/10.1111/j.1365-246X.1968.tb00184.x
10. Clark DA, Schmidt PW (1986) Magnetic properties of the banded-iron formations of the Hamersley Group, WA Sydney, Australia, CSIRO Division of Mineral Physics, AMIRA Report 1638.
11. Guo WW, Li ZX, Dentith MC (2011) Magnetic petrophysical results from the Hamersley Basin and their implications for interpretation of magnetic surveys. *Aust J Earth Sci* 58: 317–333. https://doi.org/10.1080/08120099.2011.552984
12. Guo W, Powell CMA, Dentith MC, et al. (1998) Self demagnetisation corrections in magnetic modeling: some examples, *Explor Geophys* 29: 396–401. https://doi.org/10.1071/EG998396

13. Guo W, Dentith MC, Bird RT, et al. (2001) Systematic error analysis of demagnetization and implications for magnetic interpretation. *Geophysics* 66: 562–570. https://doi.org/10.1190/1.1444947
14. Trendall AF, Pepper RS (1977) *Chemical composition of the Brockman Iron Formation*, Western Australia Geological Survey.
15. Ewers WE, Morris RC (1980) *Chemical and mineralogical data from the uppermost section of the upper BIF member of the Marra Mamba Iron Formation*, Commonwealth Scientific and Industrial Research Organization, CSIRO Division of Mineralogy.
16. Ewers WE, Morris RC (1981) Studies of the Dales Gorge Member of the Brockman Iron Formation, Western Australia. *Econ Geol* 76: 1929–1953. https://doi.org/10.2113/gsecongeo.76.7.1929
17. Gilhome WR (1975) Mount Tom Price iron orebody, Hamersley Iron Province, In: Knight CL, Eds., *Economic Geology of Australia and Papua New Guinea*, Australas Inst Min Metall Mono 5: 892–898.
18. Guo W, Howard D (2000) Interpretation of the crustal structure between the Hamersley and Ashburton Basins from gravity and magnetic data in the Wyloo area, Western Australia. *Explor Geophys* 31: 33–38. https://doi.org/10.1071/EG00033
19. Morris RC (1985) Genesis of iron ore in banded iron–formation by supergene and supergene–metamorphic processes—a conceptual model, In: Wolf KH, Eds., *Handbook of strata–bound and stratiform ore deposits*, Elsevier, 73–235.
20. Kneeshaw M (1984) Pilbara iron ore classification—a proposal for a common classification for BIF-derived supergene iron ore. *Australas Inst Min Metall* 289: 157–162.
21. Harmsworth RA, Kneeshaw M, Morris RC, et al. (1990) BIF-derived iron ores of the Hamersley Province. *Australas Inst Min Metall* Mono 14: 617–642.
22. Clout JMF (2006) Iron formation-hosted iron ores in the Hamersley Province of Western Australia. *Appl Earth Sci* 115: 115–125. https://doi.org/10.1179/174327506X138931
23. White AJR, Legras M, Smith RE, et al. (2014) Deformation-driven, regional-scale metasomatism in the Hamersley Basin, Western Australia. *J Metamorphic Geol* 32: 417–433. https://doi.org/10.1111/jmg.12078
24. Perring CS (2021) Petrography of martite-goethite ore and implications for ore genesis, South Flank, Hamersley Province, Western Australia. *Aust J Earth Sci* 68: 782–798. https://doi.org/10.1080/08120099.2021.1863860
25. Johnson GR, Olhoeft GR (1984) Density of rocks and minerals, In: Carmichael RS, Eds., *CRC handbook of physical properties of rocks*, Volume III, CRC Press Inc.
26. Emerson DW (1990) Notes on mass properties of rocks—density, porosity, permeability. *Explor Geophy* 21: 209–216. https://doi.org/10.1071/EG990209
27. Price R (1996) Basement structures of the Turner Syncline region, Hamersley Province, Western Australia. The University of Western Australia, Australia.
28. Dunlop DJ, Ozdemir O (1997) *Rock magnetism*, London: Cambridge University Press.
29. Aylmer JA, Mathew PJ, Wylie AW (1978) Bulk density of stratified iron ores and its relationship to grade and porosity. *Australas Inst Min Metall* 265: 9–17.
30. Schon JH (1996) *Physical properties of rocks: fundamentals and principles of petrophysics*, Pergamon.
31. Srigutomo W, Heriyanto M, Aufa MH (2019) Gravity inversion of Talwani model using very fast simulated annealing. *J Math Fund Sci* 51: 177–190. https://doi.org/10.5614/j.math.fund.sci.2019.51.2.7

32. Rao K, Biswas A (2021) Modeling and uncertainty estimation of gravity anomaly over 2D fault using very fast simulated annealing global optimization. *Acta Geophys* 69: 1735–1751. https://doi.org/10.1007/s11600-021-00649-8
33. Li MM, Guo W, Verma B, et al. (2009) Intelligent methods for solving inverse problems of backscattering spectra with noise: a comparison between neural networks and simulated annealing. *Neural Comput Applic* 18: 423–430. https://doi.org/10.1007/s00521-008-0219-x
34. Bailer-Jones DM, Bailer-Jones CAL (2002) Modeling data: Analogies in neural networks, simulated annealing and genetic algorithms. *Model-Based Reasoning*, Boston, MA: Springer. https://doi.org/10.1007/978-1-4615-0605-8_9